Amphiboles on the join pargasite–ferropargasite

ROBERT W. CHARLES

Los Alamos Scientific Laboratory
P. O. Box 1663
Los Alamos, New Mexico 87545

Abstract

Amphiboles have been grown across the join $NaCa_2Mg_4AlSi_6Al_2O_{22}(OH)_2$–$NaCa_2Fe_4AlSi_6Al_2O_{22}(OH)_2$ on QFM and CCH$_4$ oxygen buffers to gain insight into the Fe–Mg substitution in an amphibole without the local charge imbalance caused by Na in the $M(4)$ site. Oxygen fugacity was found to have no effect upon the unit-cell dimensions of amphibole. Unit-cell parameters ($C2/m$) for amphibole grown across the series are [a, b, c(Å), β, V(Å^3)]:

Mg$_4$	9.892(1),[1]	17.941(2),	5.277(1),	105°33'(1),	902.2(3)
Mg$_3$Fe	9.904(1),	17.989(5),	5.291(2),	105°27'(1),	908.6(5)
Mg$_2$Fe$_2$	9.915(3),	18.031(7),	5.301(3),	105°24'(1),	913.6(1.0)
MgFe$_3$	9.930(5),	18.104(6),	5.320(2),	105°16'(1),	922.6(9)
Fe$_4$	9.953(5),	18.152(3),	5.330(2),	105°16'(2),	928.8(4)

No change in cell parameters is observed with temperature on a given buffer. The essentially linear trend indicates disorder of Mg and Fe in $M(1)$, $M(2)$, and $M(3)$ sites. Plagioclase and pyroxene were present in all charges. The amount ranged from a few percent to greater than 30 percent, without affecting the unit-cell parameters of coexisting amphibole.

Introduction

Pargasites are monoclinic amphiboles having high Ca, moderate Na, and high Al. The ideal chemical formula is $NaCa_2(Mg,Fe)_4AlSi_6Al_2O_{22}(OH)_2$. The structure consists of double chains of silica and alumina tetrahedra linked by $M(1)$, $M(2)$, and $M(3)$ octahedra and by the larger 6- to 8-coordinated $M(4)$ sites (Papike *et al.*, 1969). The larger 6–12-coordinated A site completes this strip of cations. In pargasite the A site, 12-coordinated, is occupied by Na whereas the two $M(4)$ sites, 8-coordinated, are occupied by Ca. The Mg, Fe, and Al^{VI} are distributed in the remaining five M sites.

No natural occurrences of the end members pargasite and ferropargasite exist. Intermediate compositions are common in metamorphosed impure limestones, fresh and metamorphosed mafic rocks, and less commonly in altered ultramafic rocks. Ferric iron substitution for octahedral aluminum is common, placing most natural pargasites in the body of

the quadrilateral bounded by the binaries pargasite–ferropargasite and magnesiohastingsite–hastingsite. Natural occurrences of pargasite with >0.9 Al^{VI} lie between $Ca_2NaMg_3FeAlSi_6Al_2O_{22}(OH)_2$ and $Ca_2NaFe_3MgAlSi_6Al_2O_{22}(OH)_2$. Amphiboles grown experimentally on the pargasite–ferropargasite pseudobinary should be compositionally comparable to natural analogues.

In contrast to pargasites, the richterite series (Charles, 1974) has one Na in $M(4)$, and the five total $M(1)$, $M(2)$, and $M(3)$ sites are occupied entirely by Mg and Fe. The local charge imbalance caused by Na in $M(4)$ is not found in pargasites. Consequently, one of the objectives of this study was to synthesize intermediate and end-member pargasites in order to contrast some of the physical properties of the two series.

Experimental procedure

Five oxide mixes were prepared along the pargasite–ferropargasite join: Mg$_4$, Mg$_3$Fe, Mg$_2$Fe$_2$, MgFe$_3$, and Fe$_4$. As a shorthand notation only the Mg and Fe will be written: $NaCa_2Mg_3FeAlSi_6Al_2O_{22}(OH)_2$ = Mg$_3$Fe. Iron was added as hematite, Al as γ-Al$_2$O$_3$,

---

[1] Parenthesized figures represent the estimated deviation *(esd)* in terms of least units cited for the value to their immediate left, thus 9.892(1) indicates an *esd* of 0.001.

996

Table 1. Average refractive indices for the pargasite series

Phase	R. I.
Pargasite(Mg_4)	1.624 ± .003
Mg_3Fe	1.655 ± .003
Mg_2Fe_2	1.672 ± .003
$MgFe_3$	1.694 ± .003
Ferropargasite(Fe_4)	1.715 ± .005

Fig. 1. Unit-cell volume *vs.* composition for pargasite grown on CCH_4 (solid line) and QFM (dashed line). 1.00 is ferropargasite. Error bars = 1σ for all figures.

Mg as periclase, Si as cristobalite, and Na as $Na_2Si_2O_5$ prepared after the method of Schairer and Bowen (1955). After the mixes were ground in an automortar for 2 hr, a portion of each mix was reduced to Fe^0 under H_2. Results were consistent regardless of the initial state of iron; only kinetics were affected.

Oxygen fugacities were buffered with solid oxygen buffers (Eugster, 1957) and the graphite–methane buffer (Eugster and Skippen, 1967). The charges were sealed with excess water in precious-metal capsules and subjected to temperature and pressure in standard cold-seal hydrothermal apparatus.

Experimental results

Microscopic examination revealed some pyroxene and plagioclase in each charge. Amounts varied from a few percent to about 30 percent by volume, depending upon the experimental conditions. Intermediate compositions did not nucleate well. Amphibole in these charges appeared as crystalline aggregates only about $5\mu m$ in diameter. Mean refractive indices of these aggregates are tabulated in Table 1.

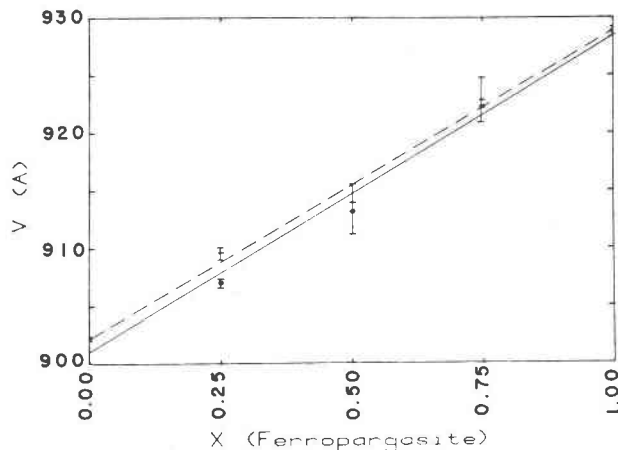The unit-cell parameters were determined using a Norelco powder X-ray diffraction goniometer. Scans of 1°/min at a strip-chart recorder rate of 1 cm/min were satisfactory to fix the peak positions of amphibole to ±0.01°, standardized against BaF_2 ($a = 6.1971\pm0.0002Å$) which has four usable reflections between 24° and 49°. BaF_2, in turn, was standardized against diamond ($a = 3.56703\pm0.00018Å$). The amphiboles ($C2/m$) were indexed and cell parameters calculated using a program developed by Appleman and Evans (1973). Twenty-five usable reflections for pargasite decreased to sixteen reflections for ferropargasite due to ambiguous indexing and poor crystallization. Pargasite and ferropargasite grown in this study are compared in Table 2 with that grown by Boyd (1959) and Gilbert (1966).

Unit-cell data for the pargasites are found in Table 3. For a given bulk composition, cell parameters are uniform with pressure and temperature. No variation was seen with oxygen fugacity (Fig. 1). Amphibole grown on CCH_4 and QFM show no difference in unit

Table 2. Unit-cell parameters of pargasite and ferropargasite

Reference	a(A)	b(A)	c(A)	β	V(A^3)
			Pargasite		
Boyd (1959)	9.906(10)	17.986(17)	5.265(8)	105°30'(8)	904.7(1.9)
This Study	9.892(1)	17.941(2)	5.277(1)	105°33'(1)	902.2(3)
			Ferropargasite		
Gilbert (1966)	9.95	18.14	5.33	105°18'	928
This Study	9.953(5)	18.152(3)	5.330(2)	105°16'(2)	928.8(4)

Table 3. Unit-cell dimensions

P (bars)	T (°C)	Duration (h)	Amphibole Yield (Percent)	Buffer	a (Å)	b (Å)	c (Å)	Beta	V (Å³)	asinβ
					Pargasite NaCa$_2$Mg$_4$AlSi$_6$Al$_2$O$_{22}$(OH)$_2$					
5000	750	527	95+	---	9.888(5)*	17.943(7)	5.280(3)	105°33'(1)	902.5(5)	
2000	750	333	95+	---	9.891(4)	17.932(6)	5.275(4)	105°30'(2)	901.5(6)	
2000	750	330	80	---	9.890(3)	17.935(6)	5.277(2)	105°32'(1)	901.9(4)	
2000	750	330	85	---	9.891(8)	17.953(22)	5.280(10)	105°38'(7)	902.8(1.0)	
2000	750	330	90	---	9.895(2)	17.939(5)	5.280(2)	105°34'(2)	902.8(3)	
2000	750	330	60	---	9.887(5)	17.940(14)	5.271(6)	105°31'(4)	900.9(9)	
1000	850	336	95+	---	9.893(2)	17.941(5)	5.276(1)	105°33'(1)	902.1(2)	
1000	850	331	99+	---	9.899(2)	17.946(3)	5.278(1)	105°35'(1)	903.1(2)	
Average					9.892(1)	17.941(2)	5.277(1)	105°33'(1)	902.2(2)	9.530
					NaCa$_2$Mg$_3$FeAlSi$_6$Al$_2$O$_{22}$(OH)$_2$					
2000	750	127	90	HMt**	9.901(3)	17.982(7)	5.296(2)	105°28'(2)	908.9(4)	
2000	750	1095	95+	QFM	9.904(3)	17.991(6)	5.290(2)	105°27'(2)	908.5(3)	
2000	625	1008	80	QFM	9.911(5)	18.006(10)	5.283(8)	105°30'(5)	908.6(1.3)	
2000	625	1008	80	QFM	9.907(5)	18.011(11)	5.288(8)	105°27'(4)	909.5(1.0)	
1000	850	1006	95	QFM	9.906(3)	18.002(6)	5.297(2)	105°26'(1)	910.6(4)	
1000	850	332	90	QFM	9.908(2)	18.003(4)	5.300(4)	105°28'(1)	911.1(2)	
2000	800	666	90	CCH$_4$	9.898(4)	17.963(10)	5.289(3)	105°27'(3)	906.4(5)	
2000	700	1015	90	CCH$_4$	9.905(2)	17.976(5)	5.286(2)	105°31'(2)	906.9(3)	
2000	750	499	90	CCH$_4$	9.898(3)	17.979(7)	5.290(2)	105°24'(2)	907.6(4)	
2000	650	120	95	IW	9.903(3)	17.979(6)	5.291(2)	105°27'(1)	908.1(3)	
Average					9.904(1)	17.989(5)	5.291(2)	105°27'(1)	908.6(5)	9.546
					NaCa$_2$Mg$_2$Fe$_2$AlSi$_6$Al$_2$O$_{22}$(OH)$_2$					
5000	650	784	60	QFM	9.919(8)	18.031(20)	5.299(4)	105°26'(4)	913.5(1.0)	
2000	750	2463	60	QFM	9.917(2)	18.048(4)	5.309(2)	105°19'(1)	916.5(3)	
2000	750	1618	85	QFM	9.906(4)	18.044(7)	5.307(2)	105°19'(2)	914.9(4)	
1000	850	1650	50	QFM	9.907(4)	18.016(8)	5.292(5)	105°25'(5)	910.7(6)	
2000	750	1015	50	CCH$_4$	9.916(5)	18.007(10)	5.294(5)	105°32'(3)	910.7(7)	
2000	700	498	85	CCH$_4$	9.925(3)	18.039(7)	5.304(2)	105°23'(2)	915.5(4)	
Average					9.915(3)	18.031(7)	5.301(3)	105°24'(2)	913.6(1.0)	9.559
					NaCa$_2$MgFe$_3$AlSi$_6$Al$_2$O$_{22}$(OH)$_2$					
5000	650	1367	90	QFM	9.918(3)	18.088(5)	5.319(2)	105°13'(1)	920.8(3)	
2000	750	427	60	QFM	9.940(4)	18.113(9)	5.326(3)	105°18'(2)	924.9(5)	
2000	625	672	95	CCH$_4$	9.927(4)	18.106(9)	5.315(3)	105°18'(2)	921.4(5)	
2000	700	1178	90	CCH$_4$	9.934(3)	18.110(16)	5.319(2)	105°15'(2)	923.1(4)	
Average					9.930(5)	18.104(6)	5.320(2)	105°16'(1)	922.6(9)	9.580
					Ferropargasite NaCa$_2$Fe$_4$AlSi$_6$Al$_2$O$_{22}$(OH)$_2$					
2000	600	368	90	QFM	9.947(3)	18.154(7)	5.332(2)	105°15'(2)	928.8(4)	
2000	700	673	95	CCH$_4$	9.958(4)	18.149(7)	5.328(2)	105°18'(3)	928.8(4)	
Average					9.953(5)	18.152(3)	5.330(2)	105°16'(2)	928.8(4)	9.602

* Parenthesized figures represent the estimated standard deviation (esd) in terms of least units cited for the value to their immediate left, thus 9.888(5) indicates an esd of 0.005.

** Buffer notation is as follows: HMt = hematite - magnetite, QFM = quartz - fayalite - magnetite, CCH$_4$ = graphite - methane, and IW = iron - wustite.
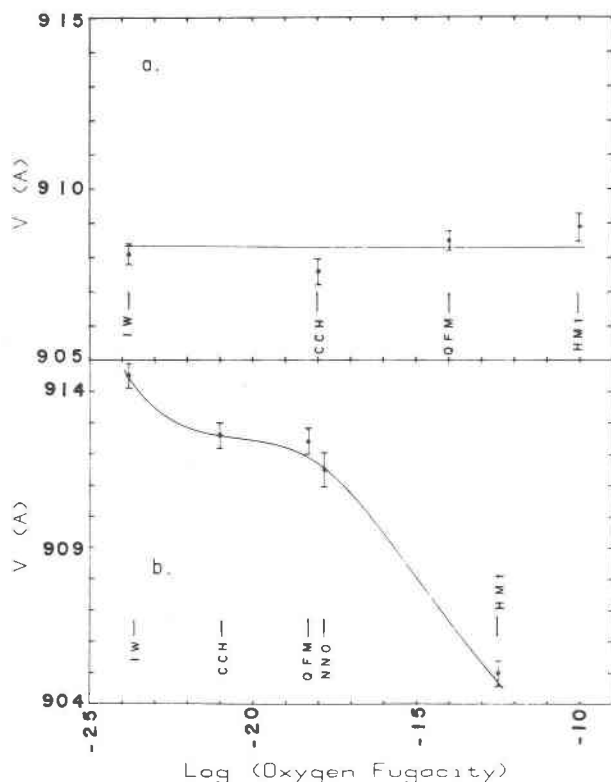
Fig. 2. (a) Unit-cell volume of pargasite $Ca_2NaMg_3FeAlSi_6Al_2O_{22}(OH)_2$ *vs.* oxygen fugacity. (b) Unit-cell volume of richterite $CaNa_2Mg_4FeSi_6O_{22}(OH)_2$ *vs.* oxygen fugacity (Charles, 1974).

QFM: $V\,(Å^3) = 26.58$ X(ferropargasite)
$$+\,902.18;\ r^2 = 0.99$$

Most experiments were done on QFM and CCH_4, but those done on HMt and IW substantiate this observation. This is in agreement with the study by Gilbert (1966), which shows essentially no variation in ferropargasite unit cell with oxygen fugacity.

Figure 2 compares the effects of oxygen fugacity on unit-cell parameters for analogous compositions in the pargasite and richterite series. The richterite is from Charles (1974). Within two sigma no trend is seen in the pargasite, whereas a dramatic decrease in cell volume is seen in the richterite with increase in oxygen fugacity.

Yields of amphibole down to about 60 percent of the charge by volume had no effect on the unit-cell parameters. Either charges with low amphibole yield nonstoichiometric pargasite with fortuitously similar cell dimensions to that of purer charges, or the amphibole is on composition. Experience with other amphibole systems indicates the latter case is more probable.

Figure 3 shows all the unit-cell data for the pargasite series. The dashed curves are similar measurements for the richterite series (Charles, 1974). All data are fitted with a linear curve by the least-squares method (Table 4). Some of the data suggest a nonlinear fit, but not at a two-sigma confidence level.

Discussion

Pargasites are more stable than richterites, $Na_2Ca(Mg,Fe)_5Si_8O_{22}(OH)_2$ (Boyd, 1959; Gilbert, 1966; Charles, 1975). A number of structural obser-

cell at the 2-sigma level. The curves are fitted by least squares to a straight line,

CCH_4: $V\,(Å^3) = 27.49$ X(ferropargasite)
$$+\,900.97;\ r^2 = 0.99$$

Table 4. Straight-line fit to unit-cell parameters $y = ax + b$, $r^2 =$ degree of fit, where $y =$ cell parameter and $x =$ mole fraction of iron-bearing end member

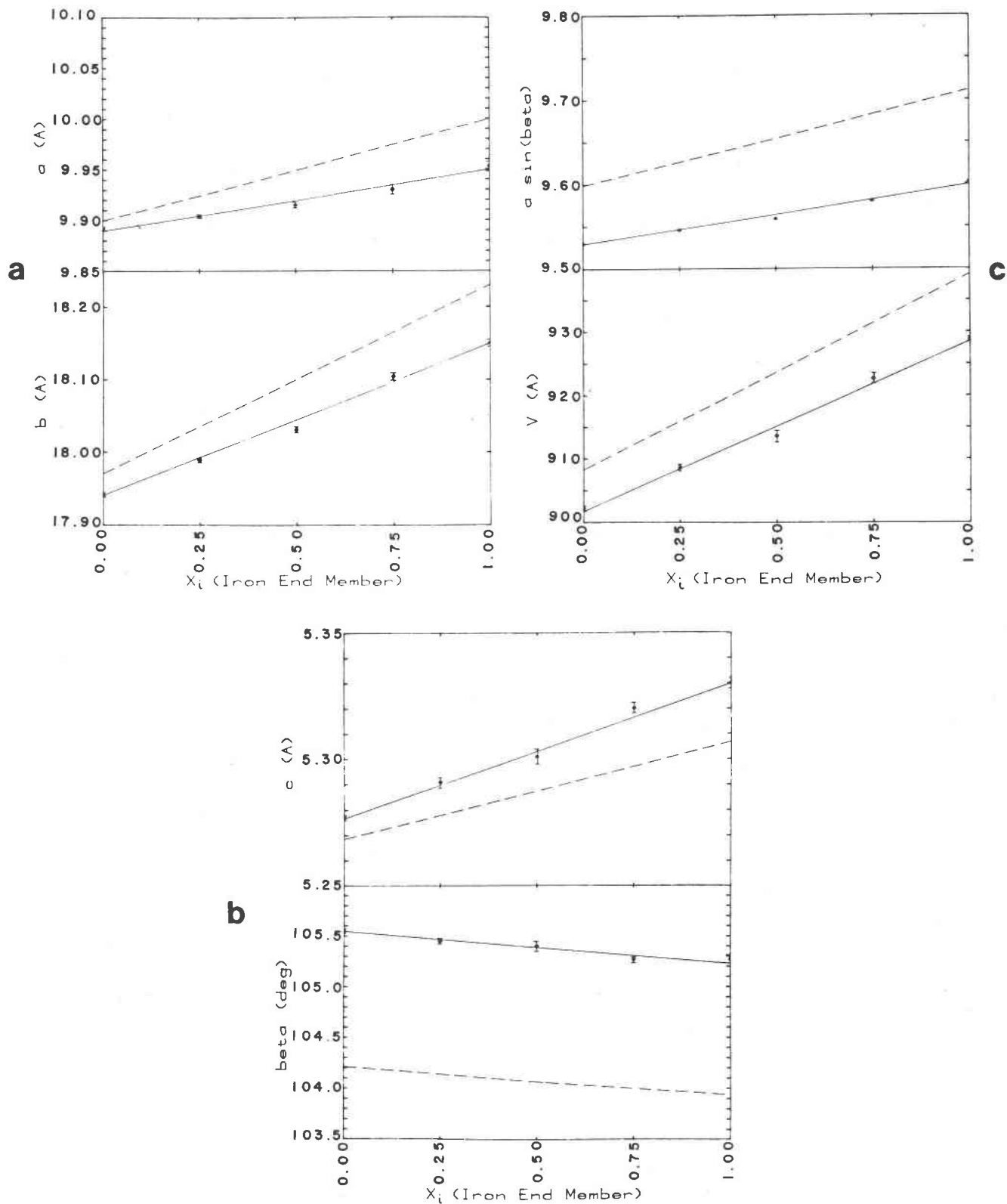| Cell Parameters	Pargasite			Richterite		
	a	b	r^2	a	b	r^2
a	0.06A	9.89A	0.97	0.10A	9.90A	0.99
b	0.21A	17.94A	0.99	0.26A	17.97A	0.99
c	0.05A	5.28A	0.99	0.04A	5.27A	0.99
β	– 18'	105° 32'	0.94	– 17'	104° 12.5'	0.99
V	$26.8A^3$	$901.8A^3$	0.99	$30.7A^3$	$908.5A^3$	1.00
asinβ	0.07A	953A	0.99	0.11A	9.60A	1.00

Fig. 3. Variation of average unit-cell parameters with composition (1.00 = ferropargasite) for pargasite (this study) and richterite grown on IW (Charles, 1974).

vations contrast the two amphibole series. The richterite structure has a local charge imbalance because one sodium must occupy an $M(4)$ site and be coordinated by six oxygens (Ghose, 1966; Whittaker, 1949, 1960). This is compensated by addition of a small amount of ferric iron in $M(2)$ which is nearest to $M(4)$ in the iron-bearing richterites. In pargasite $M(4)$ and A are occupied by Ca and Na respectively. The interior M sites contain Al and 4(Mg,Fe). Should some Na be present in $M(4)$, Al in $M(2)$ would alleviate any charge imbalance. This observation and the closer proximity of the adjacent double chains caused by a smaller mean cation size in the M sites indicate why pargasite is thermally more stable than richterite.

Figure 2 shows one effect of local charge imbalance. Pargasite shows a more uniform cell volume with respect to oxygen fugacity than does richterite. The local charge imbalance in richterite is enhanced at higher oxygen fugacities, presumably causing more ferric iron to enter $M(2)$. At the higher oxygen fugacities of the HMt buffer, richterite unit-cell parameters deviate from those observed at lower buffers toward magnesioriebeckite (Ernst, 1968), which is known to have Fe^{3+} occupying $M(2)$ (Bancroft and Burns, 1969).

The unit-cell parameters of pargasite are linear with composition in contrast to richterite (Charles, 1974). The variation in unit-cell parameters with composition can be interpreted in terms of amphibole structure. The parameters a and $a\sin\beta$ depend upon the mean size of cations linking the double chains of silica and alumina tetrahedra (Ernst, 1968; Huebner and Papike, 1970; Cameron and Papike, 1979). One would expect a linear change with addition of iron. This is observed in the pargasite series. Parameter b depends upon the occupancy of $M(4)$ and $M(2)$ which actually link the chains of silica–alumina tetrahedra. $M(4)$ is occupied by Ca and Na in all cases. If iron and magnesium are randomly distributed in $M(1)$, $M(2)$, and $M(3)$, a linear increase would result as is observed. Parameter c, chain length, reflects the occupancy of the chain and the $M(1)$ and $M(3)$ sites. Six Si and two Al are the tetrahedral cations for all pargasites. Linear increase in chain length reflects random mixing of Fe and Mg in $M(1)$ and $M(3)$. Beta mirrors changes in A site size. In all cases A is occupied by Na and possibly Ca. However, the structure around A becomes increasingly larger due to addition of iron. The net effect is that of placing a relatively smaller cation in A, causing β to decrease. Combining these effects for parga-

site, one sees a linear increase in volume within the scatter of the data.

The nonlinearities seen in richterite due to preferential filling of $M(1)$ and $M(3)$ with ferrous iron over $M(2)$ are not seen in the pargasites. A more complete discussion of richterite unit-cell parameter is presented in Charles (1974).

References

Appleman, D. E. and H. T. Evans, Jr. (1973) Indexing and least squares refinement of powder diffraction data. *Natl. Tech. Inf. Serv., U.S. Dep. Commerce, Springfield, Virginia.* Document PB-216 188.

Bancroft, G. M. and R. G. Burns (1969) Mossbauer and absorption spectral study of alkali amphiboles. *Mineral. Soc. Am. Spec. Pap., 2,* 137–148.

Boyd, F. R. (1959) Hydrothermal investigations of amphiboles. In P. H. Abelson, Ed., *Researches in Geochemistry,* p. 377–396. Wiley, New York.

Cameron, M. and J. J. Papike (1979) Amphibole crystal chemistry: a review. *Fortschr. Mineral., 57,* 28–67.

Charles, R. W. (1974) The physical properties of the Mg–Fe richterites. *Am. Mineral., 59,* 518–528.

———— (1975) The phase equilibria of richterite and ferrorichterite. *Am. Mineral., 60,* 367–374.

Ernst, W. G. (1968) *Amphiboles.* Springer-Verlag, New York.

Eugster, H. P. (1957) Heterogeneous reactions involving oxidation and reduction at high pressures and temperatures. *J. Chem. Phys., 26,* 1760–1761.

———— and G. B. Skippen (1967) Igneous and metamorphic reactions involving gas equilibria. In P. H. Abelson, Ed., *Researches in Geochemistry,* p. 492–520. Wiley, New York.

Ghose, S. (1966) A scheme of cation distribution in amphiboles. *Mineral. Mag., 35,* 46–54.

Gilbert, M. C. (1966) Synthesis and stability relations of the hornblende ferropargasite. *Am. J. Sci., 264,* 698–742.

Huebner, J. S. and J. J. Papike (1970) Synthesis and crystal chemistry of sodium–potassium richterite, $(Na,K) NaCaMg_5Si_8O_{22}(OH,F)_2$: a model for amphiboles. *Am. Mineral., 55,* 1973–1992.

Papike, J. J., M. Ross and J. R. Clark (1969) Crystal chemical characterization of clinoamphiboles based on five new structure refinements. *Mineral. Soc. Am. Spec. Pap., 2,* 117–136.

Schairer, J. F. and N. L. Bowen (1955) The system $K_2O–Al_2O_3–SiO_2$. *Am. J. Sci., 253,* 681–745.

Whittaker, E. J. W. (1949) The structure of Bolivia crocidolite. *Acta Crystallogr., 2,* 312–317.

———— (1960) The crystal chemistry of the amphiboles. *Acta Crystallogr., 13,* 291–298.